ISSN: 1813-4890

Error Analysis and Compensation of On-Machine Measurement Probe

Yongtao Yin, Hao Wu

School of Artificial Intelligence Hubei University, Wuhan 430415, China

Abstract

On-machine measurement technology enables the inspection of dimensional and geometric features without removing the workpiece, which is of great significance for improving machining efficiency and reducing errors caused by repeated clamping. However, due to factors such as machine tool motion accuracy, probe structural characteristics, and the measurement environment, certain errors still exist in on-machine measurement results, among which probe error has a particularly direct influence on measurement accuracy. Focusing on the error issues of trigger probes in on-machine measurement, this study analyzes the formation mechanisms of pre-travel error, anisotropic error, and eccentricity error. On this basis, a probe calibration and radius compensation method based on a standard sphere is investigated. By establishing a sphere-fitting model, the equivalent radius of the probe is obtained, and combined with calibration data under different surface normal directions, a bilinear interpolation algorithm is employed to realize probe radius compensation in arbitrary directions. Finally, taking a standard sphere as the experimental object, a comparative analysis of the measurement results before and after compensation is carried out. The results show that the average diameter error of the standard sphere is significantly reduced after compensation, which verifies that the proposed method can effectively improve the accuracy of on-machine measurement.

Keywords

On-machine measurement; Trigger probe; Error analysis; Standard sphere calibration; Radius compensation; Bilinear interpolation.

1. Introduction

With the development of CNC machining toward higher precision and higher efficiency, traditional offline inspection methods, which require repeated clamping and involve long inspection cycles, have become increasingly unable to meet the real-time quality control requirements of complex part machining processes[1]. On-machine measurement technology integrates the measurement process directly into the CNC machining environment, enabling the inspection of dimensional and geometric errors on site, and therefore has high application value in modern manufacturing[2].

However, due to the complex environment of on-machine measurement and the varying geometries of the workpieces being measured, ensuring measurement accuracy remains a major challenge. At the same time, the relative position between the workpiece and the measuring device is constrained during the on-machine measurement process, making the accuracy of on-machine measurement systems more difficult to control than that of offline coordinate measuring machines (CMMs)[3]. Among the many factors affecting measurement accuracy, the intrinsic accuracy of the trigger probe system is particularly critical[4].

To address the measurement errors of trigger probes, References[5] attempted to subdivide the probing process and identify the influencing factors at each stage for correction[6], thereby

ISSN: 1813-4890

reducing the overall measurement error. Reference[7] adopted a mathematical iterative method and implemented it in software to compensate for probe errors. Han Rucong, Zhang Jianfu, and others established a trigger probe radius error model using a genetic algorithm–BP neural network[8]. However, the compensation accuracy was difficult to improve significantly because it depended heavily on the selected training sample data and did not sufficiently consider the influence of measurement orientation[9].

In this paper, by analyzing the components of probe error and their causes, a mathematical model for probe calibration is established[10]. After comprehensively considering factors such as pre-travel error, probe anisotropy, and probe eccentricity during the actual measurement process, a probe radius compensation method is proposed to reduce measurement error[11]. In addition, a bilinear interpolation method is employed to calculate the probe radius compensation values for different surface normal directions, thereby improving the measurement accuracy of the on-machine measurement system[12].

2. Main Sources of Probe Errors in On-Machine Measurement

2.1. Pre-travel Error

During on-machine measurement, the probe moves along a predetermined path to the target measuring position under the control of the CNC system. When the stylus comes into contact with the workpiece surface and reaches the preset trigger force, the internal mechanism of the probe is activated, generating a trigger signal. This signal is transmitted to the CNC system through the interface, while a latch signal is generated simultaneously to record the current machine coordinates. The CNC system then stops the feed motion of the machine tool and completes the latching and storage of the measurement data, thereby accomplishing one measurement cycle.Figure 1 shows the measurement process of the probe on a standard sphere together with the timing relationship during the probe triggering process, including the correspondence among the probe motion state, the trigger signal, and the latch signal.

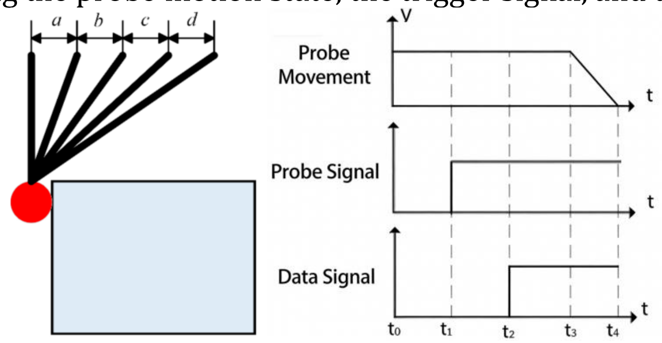

Fig.1 Timing Diagram of Probe Triggering

In trigger-type measurement, coordinate recording is not completed at the instant when the stylus contacts the workpiece. Instead, it is a continuous process involving trigger generation, signal transmission, system response, and machine deceleration. After the stylus first contacts the workpiece surface, the probe's internal triggering mechanism requires a certain amount of time to output a trigger signal. During this period, the machine tool continues moving at the original feed rate, resulting in a displacement deviation caused by pre-travel. The trigger signal is then transmitted to the CNC system, and before it is received and recognized, the relative displacement between the stylus and the workpiece continues to accumulate.

After the receiver detects the trigger signal, further processing is still needed before the measurement coordinates can be latched, which introduces an additional response delay. During this time, the machine tool remains in motion, causing the actual latched position to deviate further from the ideal contact position. After coordinate recording is completed, the machine gradually decelerates to a stop, and a certain amount of overtravel may occur. Although this usually does not directly affect the recorded coordinates, excessive overtravel may change the stress state of the stylus and influence the stability of subsequent measurements.

Thus, pre-travel error is closely related to the dynamic response of the probe after contact. From the moment the stylus contacts the workpiece until the CNC system recognizes the trigger signal and latches the current coordinates, the machine tool continues moving at the preset feed rate. The additional displacement generated during this interval constitutes the pre-travel error, which can be expressed as:

$$\eta = \eta_1 + \eta_2 + \eta_3 = v \times (t_3 - t_0) \tag{1}$$

Where v denotes the current feed speed of the probe. As can be seen from Equation (1), the pre-travel error is directly related to the time delay and the feed speed. When the probe feed speed increases, the additional displacement generated within the same response time also increases accordingly, thereby aggravating the pre-travel error. Conversely, if the feed speed is too low, although it helps reduce the additional displacement caused by dynamic effects, it will prolong the overall measurement process and reduce measurement efficiency .Therefore, in actual measurement, it is necessary to strike a balance between accuracy and efficiency and to select the probe feed speed reasonably.

In addition to feed speed and time delay, the pre-travel error is also related to the structure of the stylus itself and the contact condition. According to Equations (2) and (3), factors such as elastic deformation of the stylus, contact deformation, and displacement offset during the probing process also affect the magnitude of the error. Their relationship can be expressed as follows:

$$\mathrm{W} = \mathrm{W_a}(\phi, \theta) + \mathrm{W_b}(\phi, \theta) + \mathrm{W_c}(\phi, \theta) \tag{2}$$

$$\Delta \mathrm{d} = \Delta\alpha \cdot \mathrm{l_p} \tag{3}$$

Where $\mathrm{W_a}$ represents the elastic deformation parameter of the probe stylus itself, $\mathrm{W_b}$ denotes the deformation generated when the probe comes into contact with the workpiece, and $\mathrm{W_c}$ refers to the displacement of the stylus, while Δd represents the alignment error. In addition, θ and ϕ denote the azimuth angle and polar angle at the top of the probe, respectively, $\Delta\alpha$ is the deflection angle of the stylus, and $\mathrm{l_p}$ is the effective length of the stylus. These parameters together constitute a mathematical model describing the deformation and displacement of the stylus, providing a basis for understanding and quantifying the errors generated during the measurement process.

2.2. Probe Anisotropic Error

The probe contains three pairs of contact elements uniformly distributed on the same horizontal plane, and these three pairs are connected in series. When any one pair of contacts is disconnected, the probe generates a trigger signal, as shown in Figure 2. Owing to this structural arrangement, contacts from different directions cause different contact pairs to bear the load and disconnect first, resulting in variations in the trigger displacement of the probe along different measuring directions. Therefore, when the probe contacts the workpiece from different orientations, the pre-travel is not exactly the same. The variation in pre-travel caused by differences in measuring direction, and the resulting deviation in measurement results, is referred to as the anisotropic error of the probe. As a structural error inherent to trigger probes,

ISSN: 1813-4890

anisotropic error is closely related to the measuring direction and is particularly evident in multi-directional measurement, as well as in roundness and sphericity measurement.

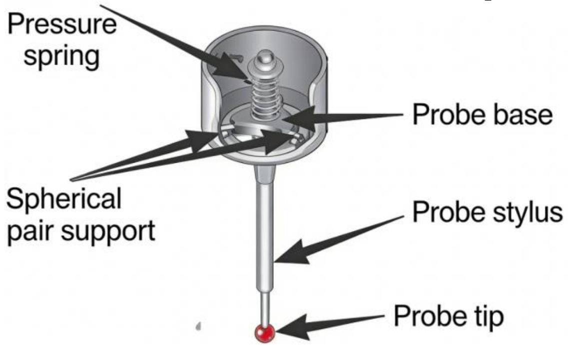

Fig.2 Schematic Diagram of the Internal Structure of the Probe

2.3. Eccentricity Error

In actual measurement, factors such as overtravel impact, plastic deformation of the stylus, and installation error may prevent the probe centerline from remaining strictly coaxial with the spindle axis. When an offset exists between them, the actual spatial position of the stylus tip deviates from its theoretical position, thereby introducing additional measurement error. As shown in Figure 3, when the probe is rotated by 180° from its original position, the stylus tip should theoretically move to a symmetrical position. However, due to the presence of eccentricity, the actual positions before and after rotation do not coincide. This positional deviation may accumulate during multi-directional measurement, thereby reducing measurement accuracy.

To reduce probe eccentricity error, the coaxiality of the probe should be calibrated with high-precision instruments such as a dial indicator when the probe is first installed or when the stylus is replaced, so as to ensure that the probe centerline coincides with the spindle axis as closely as possible. At the same time, during measurement, the probe should contact the workpiece from the same orientation as much as possible to reduce the additional error caused by changes in direction.

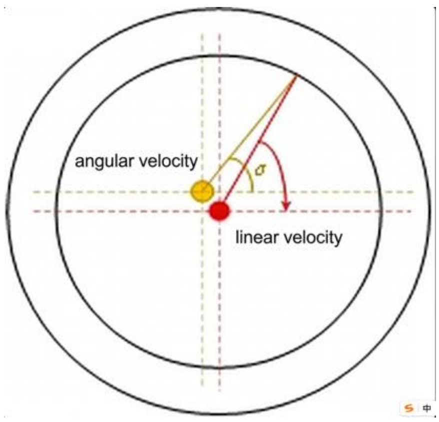

Fig.3 Schematic Diagram of Eccentricity Error

3. Probe Calibration and Compensation Principles

3.1. Importance of Probe Calibration

To reduce the influence of the probe’s structural characteristics on the measurement results, the probe usually needs to be calibrated before formal measurement in order to obtain its geometric parameters.

During on-machine measurement, when the probe approaches a measuring point along the normal direction of the workpiece surface, its working process can be simplified as the model shown in Figure 4. The machine tool drives the probe to move, and a contact force is generated after the stylus tip touches the workpiece surface. As the displacement increases and the trigger condition is satisfied, the probe outputs a trigger signal. At the triggering instant, the system latches the current machine coordinates and records them through the data acquisition module.

It should be noted that the coordinates recorded by the CNC system correspond to the probe ball center position O′, rather than the actual contact point C. Since there is a geometric offset equal to the ball radius rrr between the probe ball center and the workpiece surface, the ball center coordinates should be compensated along the surface normal in the measuring direction. By subtracting (or adding) the probe radius r in the corresponding direction, the spatial coordinates of the actual contact point can be obtained .

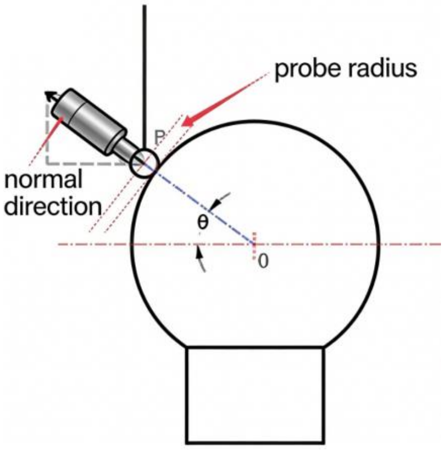

Fig.4 Schematic Diagram of the Probe Measuring the Workpiece

3.2. Mathematical Model for Probe Calibration

As discussed above, the measurement coordinates recorded by the CNC system correspond to the center position of the probe ball rather than the actual measurement point on the workpiece. Therefore, a geometric offset caused by the probe radius rrr exists between the two. To correct this deviation, the probe must be calibrated and an appropriate mathematical model must be established. In the calibration process, a standard sphere is usually used as the reference object. By collecting the spatial coordinate data of multiple measurement points on its surface and applying a sphere-fitting method, the center coordinates of the standard sphere and the equivalent radius of the probe can be determined. In this way, both the probe radius parameter and the spatial positional relationship of the system can be identified, thereby enabling radius compensation for the original measurement data.

This method uses the standard sphere as a geometric reference and improves the accuracy of parameter estimation through computational approaches such as least-squares fitting, thereby enhancing the measurement performance of the probe and ensuring the accuracy and consistency of the measurement results. The spatial equation of the sphere is shown in Equation (4).

$$(x-x_0)^2+(y-y_0)^2+(z-z_0)^2=R^2 \tag{4}$$

Where R denotes the radius of the sphere, and (x_0,y_0,z_0) represents the coordinates of the sphere center. According to spatial geometry, at least four non-coplanar measurement points are theoretically required to determine the sphere center position and the sphere size parameters. However, in actual calibration, an individual measurement point may be affected by random errors or systematic errors. Therefore, relying only on the minimum number of points makes it difficult to guarantee the stability and accuracy of the results. To improve calibration accuracy and reduce the influence of single-point errors on the overall results, the

number of measurement points should generally be increased appropriately. When a sufficient number of measurement points are collected, the least-squares method can be used to fit the sphere equation. By minimizing the sum of the squared distances from all measurement points to the fitted sphere surface, the sphere center coordinates and diameter parameters can be determined. This method can effectively improve the accuracy and stability of parameter estimation, thereby enhancing the reliability of probe calibration results.
By expanding the sphere equation, the following form can be obtained:

$$x^2+y^2+z^2-2(xx_0+yy_0+zz_0)+(x_0^2+y_0^2+z_0^2-R^2)=0 \tag{5}$$

Given that x, y, and z are known, Equation (5) can be regarded as a quaternary quadratic equation with respect to (x_0,y_0,z_0) and R. Let the coordinates of the measured points be defined as pi(xi，yi，zi), i=1,2,3…N. According to the least-squares method, the objective function can be written as:

$$F(x_0,y_0,z_0,R)=\sum_{i=1}^{N}[x_i^2+y_i^2+z_i^2-2(x_ix_0+y_iy_0+z_iz_0)+(x_0^2+y_0^2+z_0^2-R^2)]^2 \tag{6}$$

When the values of (x_0,y_0,z_0) are sufficiently small, let $C = x_0^2+y_0^2+z_0^2-R^2$. Then, the above equation can be transformed into Equation (7):

$$F(x_0,y_0,z_0,C)=\sum_{i=1}^{N}[x_i^2+y_i^2+z_i^2-2(x_ix_0+y_iy_0+z_iz_0)+C]^2 \tag{7}$$

According to the extremum principle, for FFF to reach its minimum value, the following conditions must be satisfied: $\frac{\partial F}{\partial x_0}=0$，$\frac{\partial F}{\partial y_0}=0$，$\frac{\partial F}{\partial z_0}=0$, $\frac{\partial F}{\partial C}=0$.By taking the partial derivatives of the objective function and rearranging the results, the following system of equations can be obtained:

$$\begin{bmatrix} 2\sum_{i=1}^{N}x_i^2 & 2\sum_{i=1}^{N}x_i\,y_i & 2\sum_{i=1}^{N}x_i\,z_i & -\sum_{i=1}^{N}x_i^2 \\ 2\sum_{i=1}^{N}x_i\,y_i & 2\sum_{i=1}^{N}y_i^2 & 2\sum_{i=1}^{N}y_i\,z_i & -\sum_{i=1}^{N}y_i^2 \\ 2\sum_{i=1}^{N}x_i\,z_i & 2\sum_{i=1}^{N}y_i\,z_i & 2\sum_{i=1}^{N}z_i^2 & -\sum_{i=1}^{N}z_i^2 \\ -\sum_{i=1}^{N}x_i^2 & -\sum_{i=1}^{N}y_i^2 & -\sum_{i=1}^{N}z_i^2 & N/2 \end{bmatrix} \begin{bmatrix} x_0 \\ y_0 \\ z_0 \\ C \end{bmatrix} = \begin{bmatrix} \sum_{i=1}^{N}x_i\,(x_i^2+y_i^2+z_i^2) \\ \sum_{i=1}^{N}y_i\,(x_i^2+y_i^2+z_i^2) \\ \sum_{i=1}^{N}z_i\,(x_i^2+y_i^2+z_i^2) \\ -\frac{1}{2}\sum_{i=1}^{N}(x_i^2+y_i^2+z_i^2) \end{bmatrix} \tag{8}$$

With the aid of numerical computation methods, the measured points collected on the surface of the standard sphere can be fitted to a sphere, thereby obtaining the sphere center coordinates (x_0,y_0,z_0) and the fitted radius R of the standard sphere. Since the probe actually records the spatial position of the probe ball center rather than the true contact point with the surface of the standard sphere, the fitted radius contains the effect of the probe ball radius. By comparing the fitted radius with the known actual radius of the standard sphere, the equivalent radius of the probe can be obtained; that is, the equivalent radius of the probe can be expressed as the difference between the fitted radius R and the actual radius of the standard sphere.

In the process of determining the parameters of the standard sphere, the estimation accuracy of the sphere center coordinates directly affects the subsequent radius compensation results. If the coordinate values of the original measurement data are relatively large, or if the distribution of the measured points is not ideal, direct fitting may affect the stability of the solution. Therefore, the N measured points can first be used for preliminary fitting to obtain an approximate sphere center position. Then, taking this approximate sphere center as the new reference origin, the coordinates of all measured points are translated accordingly. After the coordinate transformation, sphere fitting is performed again in the new local coordinate system, which can reduce numerical calculation errors and improve the solution accuracy of the sphere center coordinates and radius parameters.

When the measured points are relatively uniformly distributed over the surface of the standard sphere, the above stepwise fitting method can generally provide more stable calculation results. After the parameter estimation in the local coordinate system is completed, the sphere center coordinates are transformed back to the original coordinate system through inverse transformation, so that the true spatial position of the standard sphere and its corresponding radius parameters can be obtained [35].

After sphere fitting is completed, the measurement results can be further analyzed according to the deviations of each measured point from the fitted sphere surface. By calculating the geometric difference between the actual measured points and the fitted sphere surface, the error value of each measured point can be obtained, as expressed in Equation (9).

$$\sigma_i = \sqrt{(x_i - x_0)^2 + (y_i - y_0)^2 + (z_i - z_0)^2} - R \quad (i = 1, \cdots, N) \tag{9}$$

By calculating the fitting error using Equation (9), the standard error can be further obtained.

$$\sigma_{\text{st}} = \sqrt{\sum_{i=1}^{N} \left(\sigma_i - \sum_{i=1}^{N} \sigma_i / N \right)^2 / N} \quad (i = 1, \cdots, N) \tag{10}$$

The final fitting result is evaluated according to the value of the calculated standard deviation to determine whether the fitting quality meets the required criteria. If σ_{st} is too large, multiple points should be reselected from all measured points for a new round of calculation. Conversely, if σ_{st} is sufficiently small, the obtained fitting result can be regarded as acceptable.

3.3. Modeling of the Probe Measurement Process

During standard sphere calibration, the probe gradually approaches the sphere surface along the direction opposite to the surface normal at the measurement point P on the standard sphere until a trigger signal is generated, as shown in Figure 5. It should be noted that the coordinates ultimately recorded by the CNC system are not those of the actual contact point between the probe and the standard sphere surface, but rather the position of the probe ball center at the triggering instant. Therefore, to obtain the true spatial coordinates of the measured point, probe radius compensation must be applied to the original measurement data.

According to the traditional probe calibration method, it is usually sufficient to select at least four non-coplanar measurement points on the surface of the standard sphere and solve the corresponding mathematical model to obtain the probe radius compensation value. From a geometric point of view, this compensation value can be regarded as a constant parameter. However, in actual measurement, probe errors are not entirely ideal or uniformly distributed, and the results are often affected by factors such as probe eccentricity, directional anisotropy, and measurement feed speed. Therefore, if the probe radius compensation is still treated as a single constant, it is often difficult to accurately reflect the actual error characteristics under different probing directions, thereby affecting the compensation effect.

To address this issue, this paper improves the traditional calibration method. By selecting a number of representative measurement points on the surface of the standard sphere for calibration, the probe radius compensation values under different probing directions are determined separately, thereby establishing the relationship between the compensation value and the probing direction, namely the surface normal direction. Furthermore, these discrete calibration results are used to construct a direction-dependent compensation map, and a bilinear interpolation method is adopted to calculate the probe compensation value for an arbitrary probing direction. With this method, the probe radius compensation is extended from a fixed constant to a direction-dependent variable, which can better characterize the directional error features of the probe in actual measurement and improve the rationality of the compensation result and the measurement accuracy.

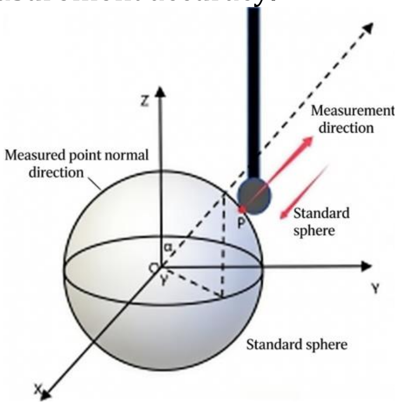

Fig.5 Schematic Diagram of the Probe Measurement Model

3.4. Probe Radius Compensation Principle

The basic idea of the bilinear interpolation method is to use the probe radius compensation values calibrated at several known surface normal directions to estimate the equivalent radius compensation for an arbitrary direction. To achieve this, it is first necessary to arrange a certain number of calibration points on the surface of the standard sphere, obtain the compensation data for different directions through actual measurement, and store these discrete results as the basis for subsequent interpolation calculations .

In this study, a Marposs G25 probe was used, and a standard sphere with a diameter of 40 mm was selected as the calibration object. The calibration points were arranged as follows: along the elevation direction, one ring of measurement points was set at every 22.5° interval, and on each ring, 8 points were uniformly distributed along the azimuth direction. The number of measurement points and the angular interval can be adjusted according to actual measurement requirements in order to achieve a balance between calibration efficiency and compensation accuracy. In the experiment, the probe feed speed was set to 50 mm/min. The distribution of calibration points on the surface of the standard sphere is shown in Figure 6.

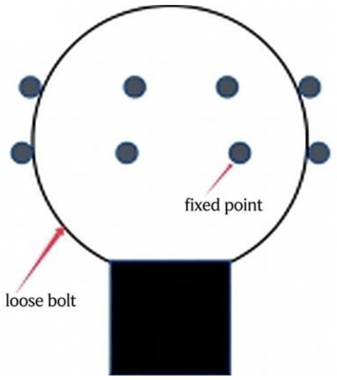

Fig.6 Schematic Diagram of Calibration Points on the Standard Sphere

After the standard sphere calibration is completed according to the above method, the probe radius compensation values corresponding to each calibrated surface normal direction can be obtained, as listed in Table 1. It can be seen from the table that the compensation values required in all directions are smaller than the nominal radius of the probe, and that the compensation value gradually decreases with the increase of the elevation angle α. This indicates that the probe radius compensation value has a clear direction-dependent characteristic.

Moreover, the compensation values are much smaller than the actual radius of the probe. In addition, the average compensation value shows a decreasing trend as the elevation angle α increases.

Table 1 Probe Radius Compensation Values at Different Angles

Azimuth θ	Elevation α						
	0	22.5°	45°	67.5°	90°	112.5°	135°
0°	2.2586	2.2398	2.2367	2.2154	2.2163	2.2179	2.2058
45°	2.2586	2.2327	2.2249	2.2046	2.1928	2.1849	2.1746
90°	2.2586	2.2351	2.2148	2.2081	2.2043	2.1886	2.1771
135°	2.2586	2.2567	2.2215	2.2162	2.2021	2.1942	2.1802
180°	2.2586	2.2571	2.2211	2.2174	2.2108	2.2023	2.1814
225°	2.2586	2.2582	2.2314	2.2079	2.2045	2.1917	2.1826
270°	2.2586	2.2570	2.2028	2.1989	2.1943	2.1856	2.1632
315°	2.2586	2.2585	2.2127	2.2058	2.1956	2.1848	2.1645
Average Value	2.2586	2.2494	2.2207	2.2093	2.2026	2.1938	2.1787

According to the previous analysis of pre-travel error, the probe feed speed is an important factor affecting the magnitude of the error. Therefore, under different measurement conditions, the feed speed should be kept as consistent as possible to ensure the effectiveness of error compensation and the stability of the measurement results.

In actual measurement, as the measurement environment and workpiece geometry change, different spatial relative positions may arise between the probe and the workpiece. According to their geometric characteristics, these typical spatial relationships can be summarized into four basic types, as shown in Figure 7.

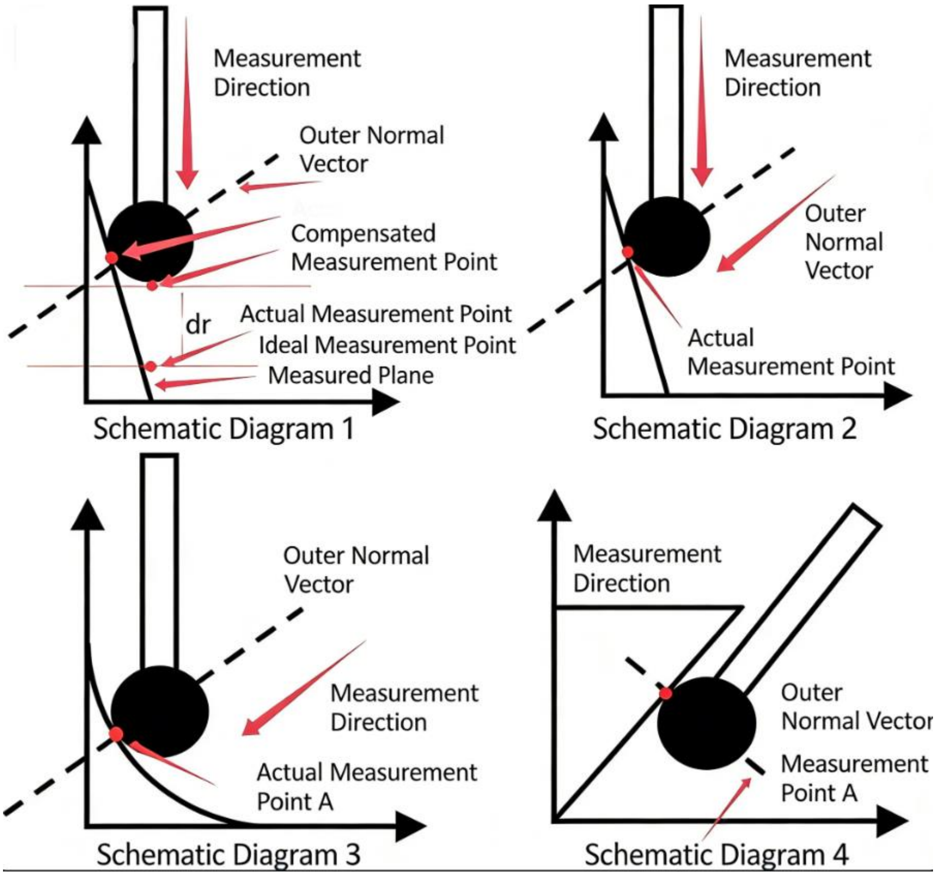

Fig.7 Schematic Diagram of Workpiece Measurement Positions

As shown in Schematic 1 of Figure 3.9, when the probe measures an inclined plane vertically downward, the actual contact point between the probe and the workpiece is point A, while the coordinate recorded by the CNC system corresponds to the probe ball center O. After radius compensation, the coordinates of the compensated point B can be obtained. However, since the measuring direction is not consistent with the surface normal direction at that point, the ideal measurement point C does not coincide with the actual contact point A. Therefore, there is still a deviation between the compensated point BBB and the ideal measurement point C, and this distance is denoted as dr. This indicates that when measuring an inclined surface, simple radius compensation alone is still insufficient to completely eliminate directional error, and further optimization of the measurement strategy or compensation algorithm is required.

As shown in Schematic 2, when the moving direction of the probe is consistent with the surface normal direction at the measured point, the probe contact point A is exactly the ideal measurement point. In this case, the coordinates obtained after radius compensation can accurately represent the position of the true measured point, and the compensation result has high accuracy, with the measurement error significantly reduced.

In the case shown in Figure 7, when the measured object is a curved surface and its radius of curvature is greater than the probe radius, the surface normal direction at the contact point between the probe and the curved surface is consistent with that at the ideal measurement point. Under this condition, radius compensation can also produce accurate results.

In addition, when the probe approaches the measured curved surface at a certain angle, if the surface normal direction at the contact point is consistent with that at the ideal measurement point, the coordinates obtained after radius compensation still maintain high accuracy. This shows that when the measuring direction is consistent with the local surface normal direction, the radius compensation method can effectively ensure the accuracy of the measured point coordinates.

Based on the above four cases, it can be concluded that in order to reduce directional error and improve measurement accuracy, the measuring direction of the probe should be made as consistent as possible with the surface normal direction of the point to be measured. Only when the measurement is carried out along the surface normal direction and the probe radius in that direction is accurately compensated can true and reliable measurement results be obtained.

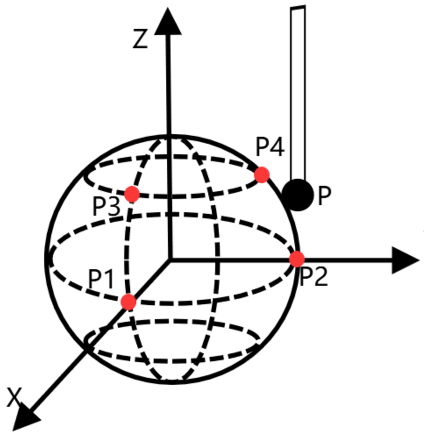

Fig.8 Schematic Diagram of the Compensation Principle

As shown in Figure 8, the compensation principle of the probe is illustrated schematically. The point to be measured, P, has a specific azimuth angle θ and elevation angle α, and is surrounded by four calibrated neighboring points, P1,P2,P3,P4. Among them, the azimuth angles of P1 and P3 are defined as θ, while those of P2 and P4 are defined as θ_2. The elevation angles of P1 and P2 are defined as α, and those of P3 and P4 are defined as α_2. Each point has a corresponding error compensation value, denoted by r_1, r_2,r_3 and r_4, respectively. Based on this information, the radius compensation value at point PPP can be calculated by using the bilinear interpolation algorithm. This method makes it possible to estimate the radius compensation at the target point from the known compensation values of its neighboring calibrated points, thereby improving measurement accuracy. The radius compensation value at point P can be calculated as shown in Equation (11):

$$\begin{aligned} r_{\alpha_1} &= (r_1 \times (\theta - \theta_1) + r_2 \times (\theta_2 - \theta))/(\theta_2 - \theta_1) \\ r_{\alpha_2} &= (r_3 \times (\theta - \theta_1) + r_4 \times (\theta_2 - \theta))/(\theta_2 - \theta_1) \\ r &= (r_{\alpha_1} \times (\alpha - \alpha_1) + r_{\alpha_2} \times (\alpha_2 - \alpha))/(\alpha_2 - \alpha_1) \end{aligned} \tag{11}$$

By mapping the probe radius compensation value rrr onto each coordinate axis according to the azimuth angle and elevation angle parameters, the compensation components along different axes can be obtained as follows:

$$\begin{aligned} d_x &= r \times \sin\alpha \times \cos\theta \\ d_y &= r \times \sin\alpha \times \sin\theta \\ d_z &= r \times \cos\theta \end{aligned} \tag{12}$$

4. Experimental Verification and Results Analysis

This experiment was conducted to verify the feasibility of the error compensation method, with a standard sphere of 30 mm diameter selected as the experimental object. The diameter of the standard sphere measured on an offline CMM was 30.0030. The experiment was carried out in the on-machine measurement environment designed in this study. Since the measurement software is still in the validation stage, the existing Huazhong–Renishaw measurement function

ISSN: 1813-4890

module was used for assisted measurement. Before and after compensation, the diameter of the standard sphere was measured at ten different measuring speeds, and each speed was tested five times. The average value was then taken to obtain the center coordinates and diameter of the standard sphere. The test environment is shown in the figure, and the obtained data are listed in the table 2.

Table 2 Standard Sphere Parameters Before and After Compensation

Trial No.	Feed Speed	Center Coordinates of the Standard			Diameter of the Standard Sphere
		x	y	z	
1 Before Compensation	30	30.1569	4.6208	-34.4529	30.0029
		30.1563	4.6201	-34.4527	30.0016
2 Before Compensation	60	30.1566	4.6208	-34.4514	30.0022
		30.1577	4.6201	-34.4521	30.0012
3 Before Compensation	90	30.1578	4.6208	-34.4526	30.0014
		30.1574	4.6208	-34.4515	30.0014
4 Before Compensation	120	30.1567	4.6218	-34.4528	30.0016
		30.1564	4.6201	-34.4520	30.0020
5 Before Compensation	150	30.1568	4.6209	-34.4528	30.0033
		30.1564	4.6201	-34.4519	30.0025
6 Before Compensation	180	30.1568	4.6219	-34.4528	30.0009
		30.1563	4.6201	-34.4529	30.0011
7 Before Compensation	210	30.1565	4.6207	-34.4515	30.0039
		30.1554	4.6203	-34.4527	30.0020
8 Before Compensation	240	30.1562	4.6207	-34.4528	30.0008
		30.1557	4.6203	-34.4531	30.0011
9 Before Compensation	270	30.1561	4.6209	-34.4525	30.0036
		30.1560	4.6205	-34.4521	30.0015
9 Before Compensation	300	30.1579	4.6208	-34.4523	30.0005
		30.1561	4.6203	-34.4527	30.0001

Analysis of the data in the table leads to the following conclusions:

(1) The sphere center coordinates before and after compensation were extracted and compared under different measuring speeds. The results show that the sphere center coordinates before compensation were (30.1568, 4.6210,35.4524), while those after compensation were (28.1563, 4.6203, 35.4521). The comparison indicates that the coordinate changes in the Y and Z directions are relatively small, suggesting that the measurement results remain generally stable in these two directions. In contrast, the change in the X direction is more obvious, indicating that the compensation has a more significant corrective effect in this direction. Overall, the compensated sphere center coordinates are closer to the nominal position, showing that the probe error compensation is effective in improving sphere center localization.

(2) As can be seen from Figure 9, the diameter measurement error of the standard sphere generally increases with the increase in probe feed speed, showing a clear positive correlation between the two. This indicates that the measuring speed has a certain influence on the triggering characteristics of the probe and the measurement results. As the feed speed increases, the dynamic error during the probe triggering process also increases, causing the measurement result to deviate further from the true value. Therefore, in practical measurement,

the relationship between measurement efficiency and measurement accuracy should be considered comprehensively, and the probe feed speed should be selected appropriately.

(3) To further evaluate the effectiveness of the compensation algorithm, a statistical analysis was carried out on the ten groups of standard sphere diameter measurements before and after compensation. The absolute deviation of each group of measurements from the nominal diameter was used, and the mean value was calculated as the evaluation index. The results show that the average diameter measurement error of the standard sphere before compensation was 1.05 μm, which decreased to 0.73 μm after compensation. The average error was reduced by 0.32 μm, corresponding to an improvement in measurement accuracy of approximately 30.47%. In particular, when the measuring speed was consistent with the calibration speed, the diameter measurement error decreased from 0.99 μm before compensation to 0.61 μm after compensation, representing an accuracy improvement of approximately 38.38%. These results demonstrate that the proposed compensation algorithm can effectively reduce the influence of probe error on the measurement results and improve the accuracy of standard sphere diameter measurement, thereby verifying the effectiveness of the proposed compensation method.

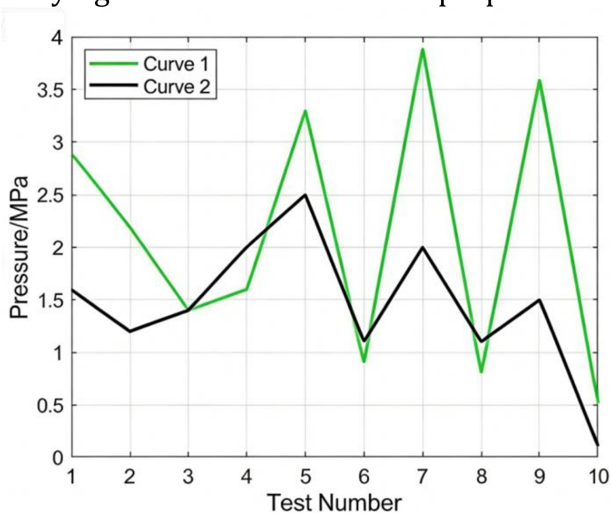

Fig.9 Comparison of Diameter Errors at Different Feed Speeds Before and After Compensation

5. Conclusion

This chapter presents the theoretical analysis and experimental verification of the probe error compensation method. First, the main sources of error in trigger probe measurement, including pre-travel error, anisotropic error, and eccentricity error, were analyzed. On this basis, a probe radius compensation method was proposed to reduce the influence of these errors on measurement results.

Next, a mathematical model for probe calibration was established, and the limitations of the traditional constant-value radius compensation method were discussed. A multi-point calibration method combined with bilinear interpolation was then proposed to calculate the probe radius compensation value for any surface normal direction. This method takes into account the combined effects of pre-travel, anisotropy, and eccentricity errors, and improves the accuracy of compensation.

Finally, comparative experiments were carried out by measuring a standard sphere at ten different speeds before and after compensation. The results show that the diameter error increases with measuring speed, while the proposed method improves the overall measurement accuracy by about 30.47%. When the measuring speed is the same as the calibration speed, the accuracy improvement reaches 38.38%. These results verify the effectiveness of the proposed method in improving the accuracy of on-machine measurement.

ISSN: 1813-4890

References

[1] Chen, Q. Q. (2012). Brief probe into online dimension measurement technology for numerical control machine. Metrology & Measurement Technique, 39(6), 37-39.

[2] Sun, Z. L. (2007). Research on the online measuring and quality evaluating system for large complex surfaces [Doctoral dissertation]. Huazhong University of Science and Technology.

[3] Marco, B., Erich, C., Christian, E., et al. (2021). Investigation on probe positioning errors affecting on-machine measurements on ultra-precision turning machines. Procedia CIRP, 101, 242-245.

[4] Qian, X. M., Ye, W. H., & Chen, X. M. (2008). On-machine measurement for touch-trigger probes and its error compensation. Key Engineering Materials, 375-376, 558-563.

[5] Zeleny, J., & Janda, M. (2009). Automatic on-machine measurement of complex parts. Modern Machinery Science Journal, 3, 92-95.

[6] Uekita, M., & Yakaya, Y. (2016). On-machine dimensional measurement of large parts by compensating for volumetric errors of machine tools. Precision Engineering, 43, 200-210.

[7] Wang, L. C., Huang, X. D., & Ding, H. (2012). Error analysis and compensation for touch trigger probe of on-machine measurement system. China Mechanical Engineering, 23(15), 1774-1778. (In Chinese)

[8] Han, R. C., Zhang, J. F., Feng, P. F., et al. (2014). Analysis and modeling of the radius error of touch trigger probes in on-machine verification system. Modular Machine Tool & Automatic Manufacturing Technique, 12, 60-64. (In Chinese)

[9] Dong, L. H., Wang, G. M., & Tong, Y. F. (2012). Calibration and practical skills of 3D-coordinate measuring head. Acta Metrologica Sinica, 33(5A), 81-83. (In Chinese)

[10] Wu, W. (2011). The error analysis and research of on-line inspection system [Master's thesis]. Wuhan University of Technology. (In Chinese)

[11] Mears, L., Roth, J. T., Djurdjanovic, D., et al. (2009). Quality and inspection of machining operations: CMM integration to the machine tool. Journal of Manufacturing Science and Engineering, 131(5), 051006.

[12] G, X. P., Y, S. H., S, C. S., et al. (2023). Contact on-machine measurement probe error correction method for optical aspheric surface ultraprecision machining. Measurement, 214, 112731.